



Catalytic ozonation not relying on hydroxyl radical oxidation: A selective and competitive reaction process related to metal–carboxylate complexes

Tao Zhang, Jean-Philippe Croué*

Water Desalination and Reuse Center (WDRC), King Abdullah University of Science and Technology (KAUST), Thuwal 4700, Saudi Arabia

ARTICLE INFO

Article history:

Received 1 April 2013

Received in revised form 13 August 2013

Accepted 14 August 2013

Available online 23 August 2013

Keywords:

Catalytic ozonation

Selectivity

Competitive degradation

Competitive adsorption

Metal–carboxylate complex structure

ABSTRACT

Catalytic ozonation following non-hydroxyl radical pathway is an important technique not only to degrade refractory carboxylic-containing organic compounds/matter but also to avoid catalyst deactivation caused by metal–carboxylate complexation. It is unknown whether this process is effective for all carboxylates or selective to special molecule structures. In this work, the selectivity was confirmed using $O_3/(CuO/CeO_2)$ and six distinct ozone-resistant probe carboxylates (i.e., acetate, citrate, malonate, oxalate, pyruvate and succinate). Among these probe compounds, pyruvate, oxalate, and citrate were readily degraded following the rate order of oxalate > citrate > pyruvate, while the degradation of acetate, malonate, and succinate was not promoted. The selectivity was independent on carboxylate group number of the probe compounds and solution pH. Competitive degradation was observed for carboxylate mixtures following the preference order of citrate, oxalate, and finally pyruvate. The competitive degradation was ascribed to competitive adsorption on the catalyst surface. It was revealed that the catalytically degradable compounds formed bidentate chelating or bridging complexes with surface copper sites of the catalyst, i.e., the active sites. The catalytically undegradable carboxylates formed monodentate complexes with surface copper sites or just electrostatically adsorbed on the catalyst surface. The selectivity, relying on the structure of surface metal–carboxylate complex, should be considered in the design of catalytic ozonation process.

© 2013 Elsevier B.V. All rights reserved.

1. Introduction

Heterogeneous catalytic ozonation is a potential oxidation technique to improve organic pollutant degradation or mineralization for surface water and wastewater treatment [1]. According to studies performed on a number of transition metal oxides and noble metals, catalytic ozonation follows either hydroxyl radical oxidation or non-hydroxyl radical oxidation pathways [1–7]. Hydroxyl radical has high reaction rate constants with most organic pollutants [8]. However, its reaction rates with saturated carboxylic-containing compounds are relatively low compared to its reaction with ozone molecule ($k_{OH} = 1 \times 10^8 - 2 \times 10^9 \text{ M}^{-1} \text{ s}^{-1}$) [8] (ineffective hydroxyl radical consumption). Ozonation and hydroxyl radical oxidation produce hydrophilic byproducts from organic matter present in water. For instance, high concentrations of carboxylates (e.g., acetate and oxalate) and keto carboxylates (e.g., pyruvate and ketomalonnate) are usually detected in natural

water subjected to ozonation and hydroxyl radical oxidation [9,10]. Carboxylates such as citrate and succinate universally present in surface water (as high as 10 mg L^{-1} have been reported), which originate from industrial wastewater effluent discharge or natural metabolites of plants, animals, and microorganisms [11–15]. Citrate is also a chloroform precursor [11] and a good analog for functional groups of humic acids to study the mechanisms of their adsorption on minerals [16]. Usually, carboxylates in water form complexes with surface metal sites of metal oxides [17]. The efficiency of catalytic ozonation relying on hydroxyl radical generation can be reduced in long term-operation, due to the formation of metal–carboxylate complexes that significantly hinder ozone–surface interaction. Therefore, the degradation of carboxylates is not only important to reduce hydrophilic byproducts [18], but also critical to avoid deactivation of the catalytic ozonation for successive operations.

Previous studies showed that non-hydroxyl radical oxidation is the major degradation pathway of carboxylates during catalytic ozonation [18–22]. The pathway relies on surface complex formation of carboxylates with active metal sites. Noble metals seem to be the most efficient in the activation of surface carboxylate complexes for ozone oxidation but low pH is always necessary to achieve efficient degradation [6]. MnO_2 , Fe_2O_3 and Co_3O_4 are

* Corresponding author at: Water Desalination and Reuse Center (WDRC), King Abdullah University of Science and Technology (KAUST), Thuwal 4700, Saudi Arabia. Tel.: +966 02 808 2984.

E-mail address: jp.croue@kaust.edu.sa (J.-P. Croué).

also active oxides in this process, but the low pH condition (≤ 3) is again required for efficient reaction [19,20,23], because H^+ is consumed during the reaction [18,21]. In our recent work, ceria significantly improved the activity of copper oxide in catalytic ozonation of oxalate at neutral pH values [7]. Moreover, it showed low metal leaching (less than $0.2 \mu\text{g L}^{-1}$ of copper was leached at the catalyst dosage of 100 mg L^{-1} at neutral pH) and high stability in repeated using. This catalyst does not promote hydroxyl radical generation from ozone, because (1) bicarbonate (a hydroxyl radical scavenger) promoted the catalytic ozonation, and (2) the degradation of atrazine (a hydroxyl radical probe compound) in the catalytic ozonation was even lower than that in ozonation alone. The ceria-supported copper oxide (CuO/CeO_2) could be a potential low cost and high efficient catalyst to promote carboxylate degradation in combination with ozone for surface water and wastewater treatment.

Thus far, all of studies on catalytic ozonation with non-hydroxyl radical pathway focused on single probe carboxylate. There is a lack of investigation on the selectivity of this oxidation process for different kinds of compounds. It is also unknown whether or not competitive reactions exist among different carboxylates during catalytic ozonation. Answering these questions would significantly improve our understanding on catalytic ozonation and help to better elaborate durable and multi-functional catalytic ozonation process for applications.

In this work, the selectivity of catalytic ozonation not relying on hydroxyl radical oxidation was studied using CuO/CeO_2 as catalyst and six ozone-resistant carboxylates (i.e., acetate, citrate, malonate, oxalate, pyruvate and succinate) as probe compounds. Additional experiments were performed to investigate competitive degradation of the probe carboxylates during catalytic ozonation. Competitive degradation was ascribed to competitive adsorption of the probes on the catalyst. The selectivity of the catalytic ozonation was correlated to the structure of surface metal–carboxylate complex. To the best of our knowledge, this is the first study showing selective and competitive reactions for catalytic ozonation.

2. Experimental

2.1. Materials and characterization

Ceria supported copper oxide (CuO/CeO_2) was prepared by immersing CeO_2 particles (prepared with a urea-hydrothermal method [6]; BET surface area of $94 \text{ m}^2 \text{ g}^{-1}$ and average particle size of $10 \mu\text{m}$) into $\text{Cu}(\text{NO}_3)_2$ solution for 24 h, drying at 120°C for 12 h, and then calcinating at 550°C for 4 h. The CuO weight percentage of the CuO/CeO_2 was determined to be 12% by ICP-MS (Agilent 7500) analysis after digestion of the catalyst with $\text{HCl} + \text{HNO}_3$ (v/v, 3:1) and HF in sequence. Energy-dispersive X-ray spectroscopy (EDX) taken on a Titan 80-300 transmission electronic microscope showed that copper dispersed well on the ceria support with surface Cu/Ce atom ratio of approximately 1:3 to 1:4 [7]. X-ray photoelectron spectroscopy (XPS) (Kratos AMICUS/ESCA 3400 spectrometer) characterization shown in our previous work [7] indicated that the oxidation state of copper on the ceria support was mainly Cu(II). The catalyst has a specific surface area of $64 \text{ m}^2 \text{ g}^{-1}$ (determined on a Micromeritics ASAP 2420 analyzer), an average particle size around $10 \mu\text{m}$ (measured on a Mastersizer 2000 laser particle size analyzer), and a pH_{pzc} of 9.1 (determined with acid–base titration). Copper oxide was prepared through calcination of copper nitrate at 550°C (same temperature as CuO/CeO_2 preparation) for 4 h. It has a specific surface area of $8.4 \text{ m}^2 \text{ g}^{-1}$, an average particle size of $6 \mu\text{m}$, and a pH_{pzc} of 9.5.

Acetic, malonic, oxalic, pyruvic, succinic and citric acids having relatively low reactivity toward ozone, were used in this

study. Their molecule structures, molecular weights, dissociation constants (pK_a) and second order reaction rate constants with ozone and hydroxyl radical were listed in Table 1.

2.2. Experimental procedure

A mass of 20 mg of catalyst was introduced into 200 mL of carboxylate solution (pH adjusted) in a 500 mL magnetically stirred glass reactor. Gaseous ozone ($27 \text{ mg O}_3 \text{ L}^{-1}$) produced from dried oxygen gas with an ozone generator (3S-A5, Tonglin Technology), was continuously introduced into the reactor through a stainless steel syringe needle (no dispenser was used to avoid any potential adsorption on the dispenser) at a flow rate of 2.0 L min^{-1} . Samples taken at predetermined time intervals were immediately filtered with $0.45 \mu\text{m}$ acetate-fiber syringe filters and then purged with pure N_2 to remove residual ozone. Filtration and purging had no impact on the carboxylate concentration.

Isothermal (20°C) adsorption was conducted at pH 7.5 without buffer addition to avoid any interference of other anions on carboxylate adsorption. Carboxylic acid solution was prepared by directly dissolving the organic acid into Milli-Q water ($18 \text{ M}\Omega \text{ cm}$, Millipore). Alkaline carboxylate solution was prepared by adding NaOH pellet into the carboxylic acid solution. Carboxylate solution of pH 7.5 was prepared by slowly dropping the alkaline carboxylate solution into the carboxylic acid solution with magnetic stirring and online pH measuring. Series of initial concentrations (0.025 – 0.5 mM for individual adsorption and 0.015 – 0.18 mM for competitive adsorption) of each carboxylate and fixed catalyst dose (2 g L^{-1}) were used for adsorption experiments. The suspension was mixed with a rotator for 36 h, and then centrifuged at 4000 rpm for 5 min. The supernatant was analyzed for residual carboxylate concentration.

2.3. Analysis

Ozone concentration in gas phase was determined with iodometric method. Aqueous ozone concentration was analyzed with a UV spectrometer (Hach 500) at 258 nm (molar adsorption coefficient = $3000 \text{ M}^{-1} \text{ cm}^{-1}$). Acetate, pyruvate and oxalate were analyzed on a Dionex ICS-3000 IC equipped with an AS-11 column (2 mm i.d.). The mobile phase, i.e., 10 mM KOH , was pumped through at a flow rate of 0.35 mL min^{-1} . Malonate, succinate, and citrate were determined on a Waters HPLC equipped with an X-Bridge column at UV wavelength of 210 nm. Diluted phosphoric acid solution ($300 \mu\text{L}$ concentrated phosphoric acid in 1 L of Milli-Q water) was used as mobile phase at a flow rate of 0.4 mL min^{-1} .

To characterize surface carboxylate complex, 150 mg of pre-ozonated oxide was mixed with 25 mL of carboxylate solution (100 mM ; pH 7.5) for 24 h. The suspension was centrifuged at 4000 rpm. The supernatant was replaced by 1 mL of Milli-Q water. After mixing, the new suspension was dropped on the crystal of a Universal ATR accessory and scanned 50 times at a resolution of 2 cm^{-1} on a PerkinElmer FTIR spectrometer (Spectrum 100). Milli-Q water was used to scan the background. It was automatically subtracted from the spectra of the samples.

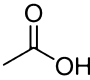
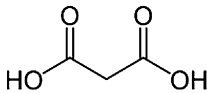
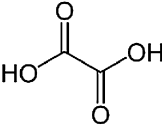
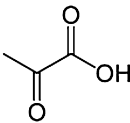
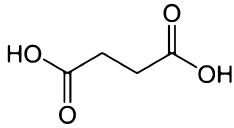
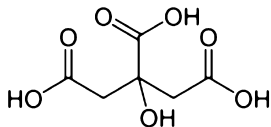
3. Results and discussion

3.1. Selectivity of catalytic ozonation

Fig. 1A and B show the removal of six carboxylates in separate solutions during ozonation alone and catalytic ozonation with CuO/CeO_2 at pH 7.5. For ozonation alone, the degradation rate of citrate was the highest (33% in 25 min) among the six compounds studied, followed by pyruvate (17%). The degradation rate of the other four carboxylates in ozonation alone ranged from 8% to 15%. In

Table 1

Characteristics of the studied organic acids: structure, molecular weight, dissociation constant, and reaction rate constant with ozone and hydroxyl radical.

Organic acid	Molecular structure	Molecular weight (g mol ⁻¹)	pK _a	k _{O₃} (M ⁻¹ s ⁻¹)	k _{•OH} (M ⁻¹ s ⁻¹)
Acetic acid		60	4.76	≤3 × 10 ⁻⁵ [24]	8.5 × 10 ⁷ [25]
Malonic acid		104	2.83; 5.69	<4 [24]	3.1 × 10 ⁷ [21]
Oxalic acid		90	1.23; 4.19	≤4 × 10 ⁻² [24]	7.7 × 10 ⁶ [18]
Pyruvic acid		88	2.39	0.025 [21]	7 × 10 ⁸ [27]
Succinic acid		118	4.21; 5.64	3 × 10 ⁻² [24]	2 × 10 ⁸ [21]
Citric acid		192	3.13; 4.74; 6.40	–	5.0 × 10 ⁷ [26]

comparison to ozonation alone, oxalate, citrate and pyruvate were effectively removed by catalytic ozonation, while the removal rates of acetate, malonate and succinate were not promoted in presence of the catalyst. As compared with ozonation alone (Fig. 1A), CeO₂ particles did not improve the removal of oxalate, citrate, and pyruvate in presence of ozone (Figure S1, Supporting Information). In contrast, O₃/CuO improved their degradation (Figure S2, Supporting Information). However, the CuO showed much lower activity than the CuO/CeO₂, which could be ascribed to its lower surface area than the CuO/CeO₂ as well as the absence of promotion effect of ceria support [7]. The results indicate that copper sites of the catalyst are active sites. These three carboxylates were removed by less than 5% during CuO/CeO₂ adsorption alone at the same dosage and contact time as used for catalytic ozonation (not shown here). Therefore, their removal can be attributed to degradation but not adsorption. The result clearly shows that the catalytic ozonation cannot universally degrade all carboxylates. This oxidation mode has strong selectivity.

It was noticed from Fig. 1A that oxalate removal rate was the fastest during the O₃/(CuO/CeO₂) oxidation with nearly 100% removal achieved within 10 min. Complete removal of citrate was achieved in 15 min. The removal rate of pyruvate was the slowest among the three catalytically degradable carboxylates. Its complete removal needed over 25 min. According to the literature (Table 1), oxalate is the least reactive species toward hydroxyl radical among the six selected probe carboxylates. However, it was most efficiently degraded during catalytic ozonation. This result confirmed that this catalytic ozonation process did not rely on hydroxyl radical oxidation, which is consistent with our previous result on catalytic ozonation of oxalate in batch experiments [7].

The degradability of the carboxylates during catalytic ozonation is not directly related to the number of carboxylate group present in the molecule. Citrate, a tricarboxylate, was less reactive than oxalate during the catalytic ozonation. Moreover, pyruvate, a

monocarboxylate was much more reactive than dicarboxylates, i.e., malonate and succinate. The presence of α-carbonyl (C=O) group in oxalate and pyruvate and α-COH group in citrate seem contributed to their degradation in the catalytic ozonation. Carboxylates with these moieties might form specific surface complexes with the catalyst active sites, leading to ready degradation by ozone.

3.2. Effect of pH

Fig. 2A and B show the influence of pH on removal rates of the six carboxylates after 10 min ozonation and catalytic ozonation. As compared with ozonation alone, the removal rates of oxalate, pyruvate and citrate were improved by catalytic ozonation in the pH range 3.0–9.2. In contrast, the removal of acetate, malonate, and succinate was not promoted by catalytic ozonation for the same pH range. This finding indicates that their low degradability is not related to their chemical form, i.e., protonated/deprotonated functional group (pK_a shown in Table 1), but possibly depends on their structure. Oxalate removal by catalytic ozonation significantly increased from 11% to 98% as solution pH was raised in the range of 3.0–7.5, while decreased to 65% as the pH was further increased to 9.2, showing again that •OH (produced by ozone-OH⁻ reaction [8]) is not a major oxidant species responsible for its degradation. The negative effect of alkaline pH on oxalate removal can be attributed to low aqueous ozone concentration at high pH (i.e., self-decomposition mechanism of molecular ozone producing •OH) (Figure S3, Supporting Information) as well as reduced affinity of the catalyst surface for oxalate because of positive surface charge decline. Degradation rates of pyruvate and citrate increased with pH in the range of 3.0–9.2, suggesting that •OH generated in water phase contributed to their oxidation. This result is reasonable considering that their reaction rate constants with •OH are much higher than that of oxalate (Table 1). The degradation rates of pyruvate and citrate at neutral pH (7.5) were quite low

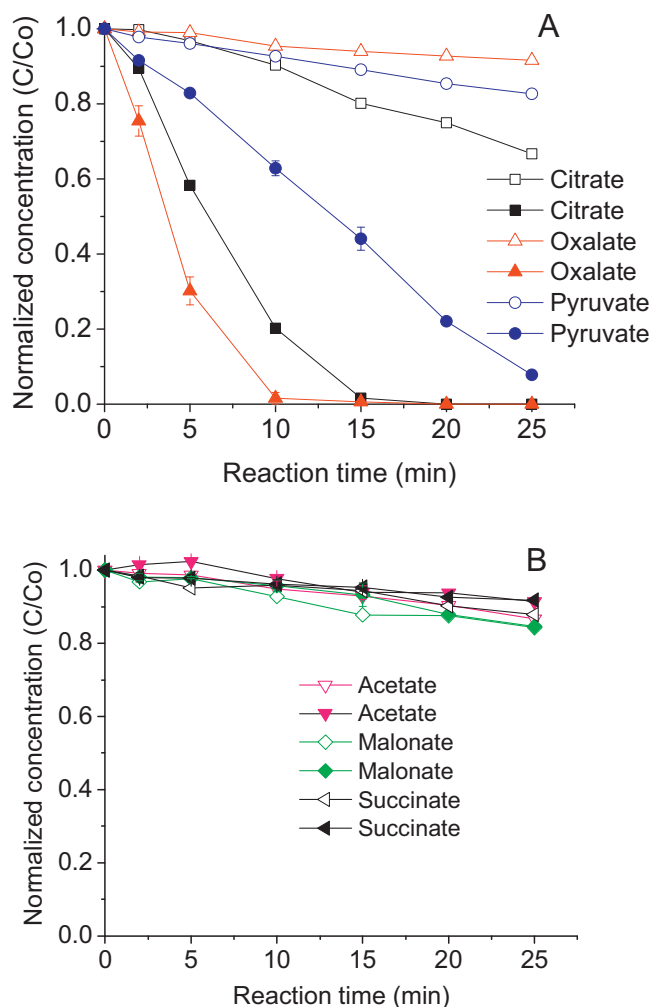


Fig. 1. Separate degradation of six carboxylates (A: citrate, oxalate and pyruvate; and B: acetate, malonate and succinate) during ozonation (open symbols) and catalytic ozonation with CuO/CeO₂ (solid symbols). Experimental conditions: ozone gas flow rate = 2.0 L min⁻¹, gaseous ozone concentration = 27 mg L⁻¹, carboxylate concentration = 0.5 mM, catalyst dose = 100 mg L⁻¹, 10 mM tetraborate buffered pH = 7.5, and *T* = 20 °C. Error bars represent standard deviation of triplicate experiments.

in ozonation alone (less than 10%), while the catalytic ozonation achieved high degradation rates for them (about 40% and 80%, respectively). As hydroxyl radical formed in the catalytic ozonation process was even less than that in ozone self-decomposition (i.e., ozonation alone) [7], the degradation of pyruvate and citrate in the catalytic ozonation is mainly due to surface reaction but not hydroxyl radical oxidation. Because removal rates of the three carboxylates are relatively low at acidic pH levels as compared with that at neutral pH, it can be concluded that the protonated form of the molecule exert low reactivity during catalytic ozonation. The protonation possibly inhibited the interaction or complexation between carboxylates and positively charged catalyst surface.

It was also noticed that the improvement of the degradation rates of oxalate, pyruvate, and citrate by catalytic ozonation, i.e., catalytic ozonation removal rate subtracted by ozonation removal rate, were higher at pH 7.5 than at other pH values. Taking into account their *pK_a* values and *pH_{pzc}* of the catalyst (9.1), the result indicates that the catalytic degradation is related to the interaction of deprotonated carboxylates with positively charged oxide surface.

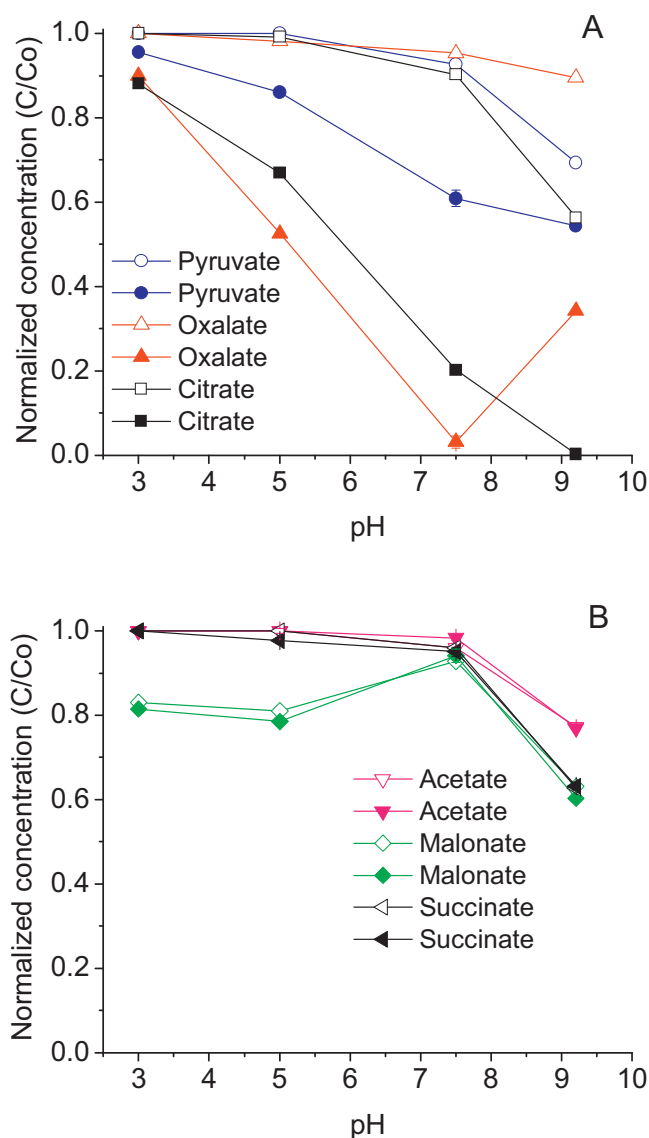


Fig. 2. Effect of pH on separate carboxylate degradation (A: citrate, oxalate and pyruvate; and B: acetate, malonate and succinate) during ozonation (open symbols) and catalytic ozonation with CuO/CeO₂ (solid symbols). Experimental conditions: ozone gas flow rate = 2.0 L min⁻¹, gaseous ozone concentration = 27 mg L⁻¹, carboxylate concentration = 0.5 mM, catalyst dose = 100 mg L⁻¹, 10 mM tetraborate buffered pH, reaction time = 10 min, and *T* = 20 °C. Error bars represent standard deviation of triplicate experiments.

3.3. Competitive reaction during catalytic ozonation

Since the degradation of pyruvate, oxalate and citrate by catalytic ozonation relies on their interaction with the catalyst surface, it is important to identify which molecule is preferentially degraded during catalytic ozonation when they coexist in a solution. This study also has application significance, as they usually coexist in natural water or wastewater as oxidation products or natural metabolites. Fig. 3 shows the removal of the three carboxylates at equivalent initial concentration in a mixture during catalytic ozonation at different pHs and initial concentrations. The degradation rate followed the order of citrate > oxalate > pyruvate (Fig. 3A). Oxalate and citrate exchanged their degradation rate order as compared with that in separate solutions (Fig. 1A), which will be explained in the next part by the preferential adsorption of citrate over oxalate on the catalyst when they coexist in a solution. It was noticed that less than 20% oxalate and 10% pyruvate

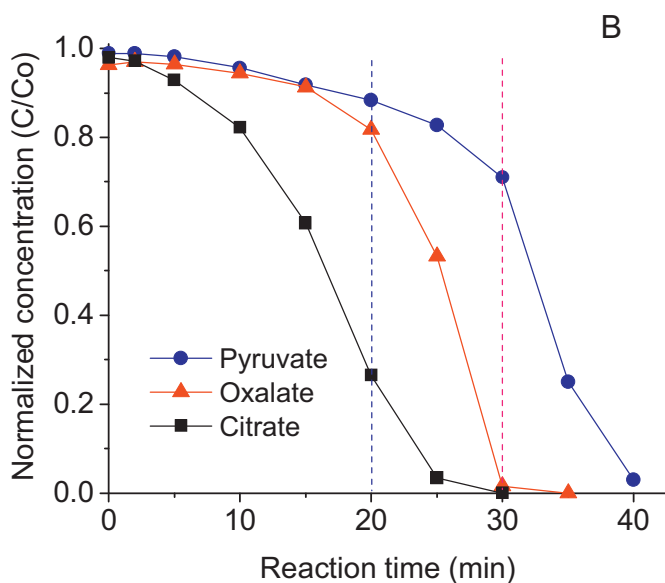
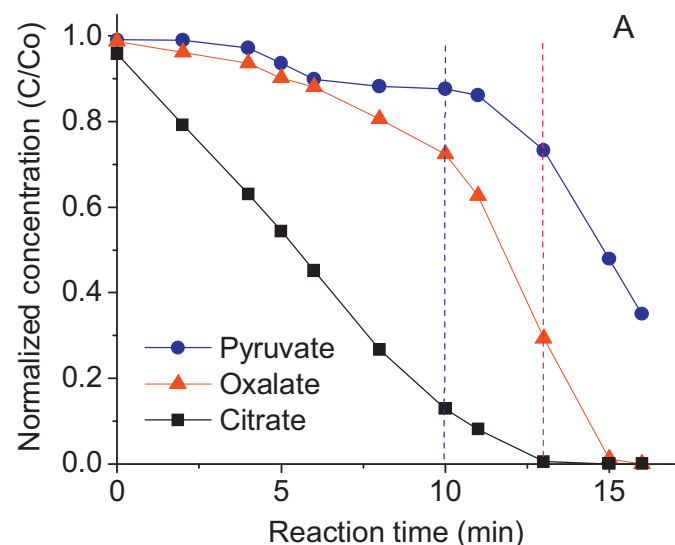


Fig. 3. Degradation of pyruvate, oxalate and citrate in mixture during catalytic ozonation with CuO/CeO₂ at (A) 0.34 mM each and pH 7.5, and (B) 0.5 mM each and pH 6.4. Experimental conditions: ozone gas flow rate = 2.0 L min⁻¹, gaseous ozone concentration = 27 mg L⁻¹, catalyst dose = 100 mg L⁻¹, 10 mM tetraborate buffered pH, and $T = 20^{\circ}\text{C}$.

were degraded before 80% citrate was degraded, and less than 25% pyruvate was degraded before 70% oxalate was degraded (Fig. 3A). Moreover, oxalate was degraded much faster when 80% citrate was degraded, and pyruvate degradation started to be significantly promoted when 70% oxalate was degraded. The results showed clearly that the three carboxylates in the mixture were degraded competitively in the catalytic ozonation. This finding was even more evident with the decrease of pH and increase of initial concentration (Fig. 3B). This competition of the carboxylates might arise from their different affinity for the catalyst surface.

Malonate and succinate were further mixed with the three catalytically degradable carboxylates. Our previous result showed that the decomposition of pyruvate in catalytic ozonation produced acetate [28]. Therefore, acetate was not introduced into the mixture. When malonate and succinate were introduced into the mixture (Figure S4, Supporting Information), they were still not

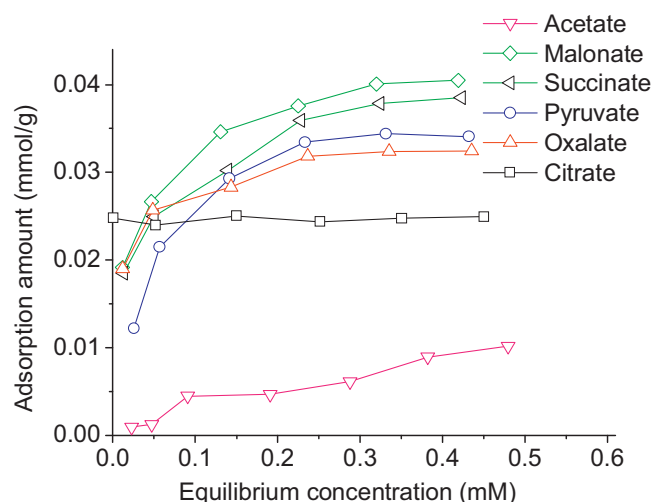


Fig. 4. Separate adsorption isotherm curves of carboxylates. Experimental conditions: oxide dose = 2 g L⁻¹, initial concentration range of each carboxylate = 0.025–0.5 mM, initial pH = 7.5, $T = 20^{\circ}\text{C}$, and contact time = 36 h.

catalytically degraded. Moreover, there was nearly no change in degradation rates and degradation order of citrate, oxalate, and pyruvate (compared with Fig. 3B), indicating that the interaction of the catalyst's active sites with the degradable carboxylates might precede over the interaction with the catalytically undegradable carboxylate.

3.4. Adsorption and competitive adsorption on the catalyst

Fig. 4 shows separate (individual solution) adsorption isotherm curves of the six carboxylates at neutral pH. Carboxylate load (i.e., initial carboxylate concentration normalized by catalyst dosage) ranged from 0.0125 to 0.25 mmol g⁻¹ for the adsorption experiments. The catalyst's adsorption capacity was highest for malonate (0.040 mmol g⁻¹) and succinate (0.038 mmol g⁻¹) and lowest for acetate (0.010 mmol g⁻¹). The three catalytically degradable carboxylates had medium adsorption on the catalyst, i.e., pyruvate (0.034 mmol g⁻¹), oxalate (0.032 mmol g⁻¹), and citrate (0.025 mmol g⁻¹). Although high adsorption capacity of the catalyst for malonate and succinate was noticed, these carboxylates were not effectively degraded during catalytic ozonation. This finding indicates that the catalysis efficiency may be related to the nature of surface oxide-carboxylate bonding or carboxylate molecular structure, but not to the adsorption capacity. Even for the three catalytically degradable carboxylates, their sorption capacity on the catalyst was not in accordance with their degradation rates.

Adsorption isotherm experiments were also conducted with mixed solutions of pyruvate, oxalate, and citrate (equal concentration of carboxylates with fixed catalyst dosage; contact for 36 h), using carboxylate load ranging from 0.0075 to 0.09 mmol g⁻¹. The catalyst showed highest adsorption capacity for citrate (0.021 mmol g⁻¹), medium for oxalate (0.011 mmol g⁻¹), and lowest for pyruvate (0.0079 mmol g⁻¹) (Fig. 5). As compared to the previous results obtained with individual carboxylates at equilibrium concentration close to 0.15 mM, the adsorption capacity for oxalate and pyruvate significantly decreased by about 65% and 70%, respectively, while much lower decrease in the adsorption for citrate (20%) was noticed. The result shows that citrate exerts more preferential sorption on the catalyst than oxalate and pyruvate in the mixture. The competitive adsorption of the three carboxylates seems responsible for their ordered degradation in mixed solutions during catalytic ozonation.

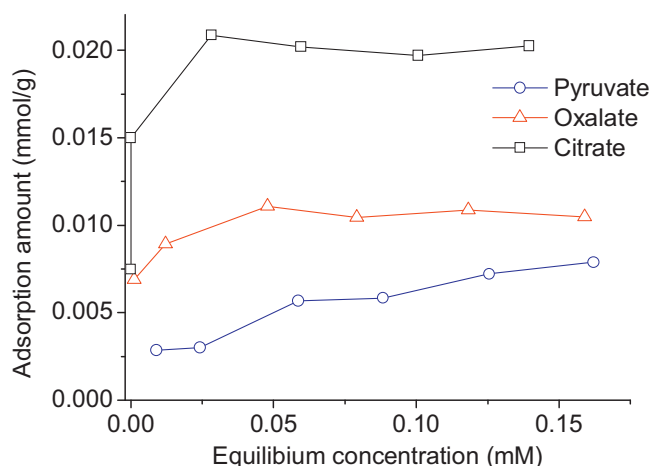


Fig. 5. Competitive adsorption isotherm curves of pyruvate, oxalate and citrate at equal initial concentrations. Experimental conditions: oxide dose = 2 g L^{-1} , initial concentration range of each carboxylate = $0.0015\text{--}0.18 \text{ mM}$, initial pH = 7.5, $T = 20^\circ \text{C}$, and contact time = 36 h.

Adsorption isotherm curves of Figs. 4 and 5 were results of 36 h catalyst/carboxylate interaction. It would be more reasonable to relate the competitive degradation to competitive adsorption at contact time and carboxylate load comparable to the catalytic ozonation conditions. The load of each carboxylate to the catalyst was 3.4 mmol g^{-1} (Fig. 3A) or 5 mmol g^{-1} (Fig. 3B) for the catalytic ozonation experiments performed with the mixed solutions. These carboxylate loads were too high to differentiate the low adsorption amounts recorded (i.e., less than 5% of the initial carboxylate dose) from experimental/analytical errors, additional short contact time adsorption experiments were then conducted with lower carboxylate loads (i.e., 0.025 and 0.1 mmol g^{-1}) (Figure S5A and S5B, Supporting Information). The adsorption rate of the three degradable carboxylates followed the order of oxalate > citrate > pyruvate at the carboxylate load of $0.025 \text{ mmol g}^{-1}$. An adsorption rate order of citrate \geq oxalate > pyruvate was observed when the carboxylate load was increased to 0.1 mmol g^{-1} . With further increase of the carboxylate load, the adsorption rate of citrate would probably be increasingly higher than the other two. When malonate and succinate were also introduced into the mixture, their adsorption onto the catalyst was much less than the three degradable carboxylates (Figure S6A and S6B, Supporting Information). It can be postulated that the catalyst adsorbs the degradable carboxylates more preferentially than the undegradable carboxylates when they coexist in a solution, which is consistent with the conclusion drawn from Figure S4. In addition, as the carboxylate load ratio increased from 0.025 to 0.1 mmol g^{-1} , adsorption rate of pyruvate was reduced, and citrate adsorption was increased much more significant than oxalate (Figure S6A and S6B, Supporting Information). The result suggests that competitive adsorption will occur in a short contact time when the carboxylate load is as high as that one used for catalytic ozonation.

On the basis of the adsorption results, it can be inferred that citrate was preferentially adsorbed on the catalyst during catalytic ozonation (high carboxylate load). The surface is accessible to oxalate when most part of citrate was degraded. Pyruvate gets more chances to interact with the catalyst surface when most of citrate and oxalate were degraded.

3.5. Surface complex structure

ATR-FTIR was used to characterize surface interactions of the six carboxylates with the catalyst pretreated with ozone oxidation. Our previous study showed that surface copper was the active site of the catalyst [7]. The ceria support functioned as promoter

of the activity of copper site by reducing its redox potential. Only interaction between copper site of the catalyst and the carboxylate can initiate the catalytic ozonation. To understand ATR-FTIR spectra of copper-carboxylate complexes, CuO calcined at the same temperature as the catalyst and pretreated with ozone oxidation was also used to study the surface interaction, which should be more relevant to the selectivity of the catalysis (absence of spectra interference of cerium-carboxylate interaction).

Fig. 6A–F shows ATR-FTIR spectra of the six carboxylates both in aqueous phase (ionic form) and in CuO/CeO₂ and CuO suspensions at pH 7.5. In aqueous phase, all of the carboxylates showed strong $\nu_{\text{as}}(\text{COO}^-)$ bands in the range of $1550\text{--}1601 \text{ cm}^{-1}$ and weaker $\nu_{\text{s}}(\text{COO}^-)$ bands in the range of $1308\text{--}1415 \text{ cm}^{-1}$. Results highlighted apparent blue-shift of $\nu_{\text{as}}(\text{COO}^-)$ band for pyruvate/(CuO/CeO₂) and malonate/(CuO/CeO₂) suspensions and red-shift for citrate/(CuO/CeO₂), pyruvate/CuO and oxalate/CuO suspensions. The $\nu_{\text{as}}(\text{COO}^-)$ band shift can be ascribed to carboxylate-metal interaction on oxide surfaces. New shoulders appeared at lower wavenumber side of the $\nu_{\text{as}}(\text{COO}^-)$ band in oxalate/(CuO/CeO₂) and citrate/CuO suspensions, which also indicates the presence of surface-bonded carboxylates besides the ionic forms in these suspensions. The shift of $\nu_{\text{s}}(\text{COO}^-)$ band was not apparent for all suspensions. An apparent adsorbed water band at 1622 cm^{-1} appeared in the spectra of acetate/(CuO/CeO₂) suspension. Broad shoulders around 1618 cm^{-1} appeared for citrate, malonate, and succinate in CuO/CeO₂ suspensions. These signals can be also ascribed to adsorbed water, as they are quite close to the band attributed to adsorbed water onto CuO/CeO₂ (Figure S7, Supporting Information).

Structures of metal-carboxylate complexes can be differentiated by applying the difference of $\nu_{\text{as}}(\text{COO}^-)$ and $\nu_{\text{s}}(\text{COO}^-)$, $\Delta\nu_{\text{as-s}}$ [29,30]. In general, complexes showing $\Delta\nu_{\text{as-s}} > \Delta\nu_{\text{as-s}}$ (ionic) can be attributed to monodentate coordination, and complexes with $\Delta\nu_{\text{as-s}} < \Delta\nu_{\text{as-s}}$ (ionic) have bidentate chelating or bridging structures. This rule was followed by a number of studies for characterization of surface complexes of carboxylates on metal oxides in water [31–34]. $\Delta\nu_{\text{as-s}}$ values for the six carboxylates both in ionic form and in oxide suspensions were calculated and listed in Table 2. In presence of CuO/CeO₂, $\Delta\nu_{\text{as-s}}$ of pyruvate and malonate increased by 11 and 4 cm^{-1} respectively as compared with their ionic forms. For oxalate and citrate, $\Delta\nu_{\text{as-s}}$ decreased by 14 and 11 cm^{-1} , respectively; no apparent change was observed for acetate and succinate. In presence of CuO, $\Delta\nu_{\text{as-s}}$ of pyruvate, oxalate, and citrate decreased by 5, 5 and 11 cm^{-1} , respectively; it slightly increased by 2 and 3 cm^{-1} for malonate and succinate, respectively; no apparent change was identified for acetate. The difference of CuO and CuO/CeO₂ in inducing decrease/increase of the $\Delta\nu_{\text{as-s}}$ can be attributed to distinct coordination nature of CeO₂ from CuO. The band shifts observed in the CuO/CeO₂ suspension would be dominated by the interaction between carboxylates with the CeO₂ support, because (1) surface molar Ce content of the catalyst is 3–4 times higher than Cu, and (2) CeO₂ can strongly interact with the carboxylate and lead to peak shift [6]. Since CeO₂ itself was not active in catalytic ozonation [6,7], its interaction with carboxylates will not directly lead to degradation. The nature of carboxylate bond to copper sites should be more relevant to their degradation activity. According to the ATR-FTIR results and the above-mentioned rule for the identification of metal-carboxylate complex structures, pyruvate, oxalate, and citrate formed bidentate chelating or bridging complexes with surface copper sites. Malonate and succinate formed monodentate coordination with the surface copper sites. The interaction between acetate and CuO surface seemed to be only electrostatic. No direct relationship can be established between the number of carboxylic group of the carboxylate molecules and the complex structure. The strong bidentate binding of pyruvate, oxalate, and citrate with surface

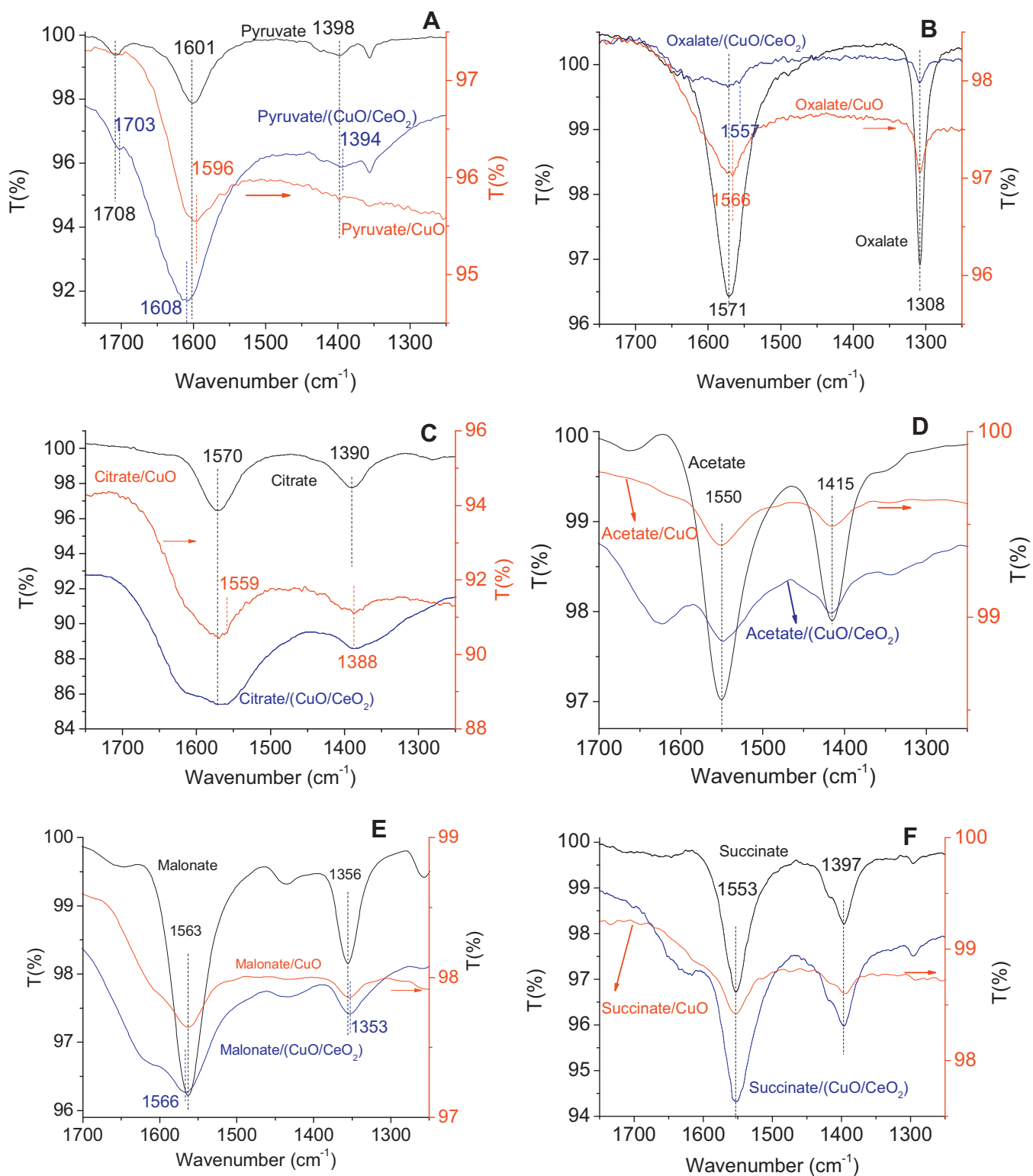


Fig. 6. ATR-FTIR spectra of carboxylates in aqueous phase and in metal oxide suspensions at pH 7.5 (A: pyruvate; B: oxalate; C: citrate; D: acetate; E: malonate; and F: succinate).

copper sites possibly arises from their α -carbonyl/ α -hydroxyl moieties. Both α -carbonyl and α -hydroxyl moieties of carboxylate are electron abstracting due to inductive effect, which increases acidity of the carboxylic acids (i.e., deprotonation). The electron abstract effect of α -carbonyl and α -hydroxyl moieties would also influence the coordination of carboxylate groups with metal

ions. It was suggested that α -hydroxycarboxylate-containing ligands preferentially form chelate coordination with divalent or trivalent metal ions like Cu(II) and Al(III) [35]. Bidentate chelating of α -carbonyl carboxylates with metal ions like Fe(II) and Cu(I) was proposed to lead to oxidative decarboxylation of carboxylates in biochemical processes [36]. Surface complexes with bidentate

Table 2Asymmetric and symmetric vibration frequencies (cm^{-1}) of carboxylate COO^- in aqueous phase and on oxide surfaces recorded by ATR-FTIR at pH 7.5.

	$\nu_{\text{as}}(\text{COO}^-)$	$\nu_{\text{s}}(\text{COO}^-)$	$\Delta\nu_{\text{as-s}}$	$\Delta\nu_{\text{as-s}}(\text{suspension}) - \Delta\nu_{\text{as-s}}(\text{ionic})$
Pyruvate	1601	1398	203	–
Pyruvate/(CuO/CeO ₂)	1608	1394	214	11
Pyruvate/CuO	1596	1398	198	–5
Oxalate	1571	1308	263	–
Oxalate/(CuO/CeO ₂)	1557 ^a	1308	249	–14
Oxalate/CuO	1566	1308	258	–5
Citrate	1570	1390	180	–
Citrate/(CuO/CeO ₂)	1559 ^a	1388	171	–11
Citrate/CuO	1559 ^a	1388	171	–11
Acetate	1550	1415	135	–
Acetate/(CuO/CeO ₂)	1548	1416	132	–1
Acetate/CuO	1551	1415	136	1
Malonate	1563	1356	207	–
Malonate/(CuO/CeO ₂)	1566	1353	213	4
Malonate/CuO	1563	1354	209	2
Succinate	1553	1397	156	–
Succinate/(CuO/CeO ₂)	1552	1396	156	0
Succinate/CuO	1553	1394	159	3

^a The $\nu_{\text{as}}(\text{COO}^-)$ band of adsorbed carboxylate was assigned to the new shoulder close to the $\nu_{\text{as}}(\text{COO}^-)$ of ionic carboxylate.

chelating or bridging structure seem more reactive toward ozone than monodentate complexes. It is a reasonable assumption, considering that high electron density (donated by the ligand) on the coordinated copper site would be more favorable for electron abstraction by ozone leading to valence increase of the coordinated copper sites. The high valent copper (Cu(III)) is not stable, which usually retrieve back to Cu(II) through an electron transfer from the coordinated carboxylate, thus leading to oxidative decarboxylation of the carboxylate [7,36]. As shown in our previous work [7], the Cu(II)/Cu(III) redox process can well explain the efficient degradation of oxalate in the catalytic ozonation with CuO/CeO₂. The degradation of pyruvate and citrate in the catalytic ozonation possibly is also initiated by the Cu(II)/Cu(III) redox process as α -carbonyl/ α -hydroxyl groups of these carboxylates facilitate the formation of similar surface bidentate Cu(II)–carboxylate complexes.

4. Conclusion

Catalytic ozonation not relying on hydroxyl radical oxidation effectively degraded carboxylates containing α -carbonyl or α -hydroxyl moieties (e.g., citrate, oxalate and pyruvate) in water but not for carboxylates without these moieties (e.g., acetate, malonate and succinate). The selectivity of the catalytic ozonation is independent on carboxylate group number of the compounds and solution pH. The catalytically degradable carboxylates were competitively degraded during the catalytic ozonation, which can be ascribed to their competitive adsorption on the catalyst. Possibly due to bidentate chelating or bridging structure of the copper–carboxylate complexes, α -carbonyl- and α -hydroxyl-containing carboxylates were selectively degraded during the catalytic ozonation. Monodentate coordination and purely electrostatic adsorption of the carboxylates to active sites of the catalyst cannot induce catalytic degradation. The bidentate coordination on the catalyst precedes over the monodentate coordination. The conclusion is only based on limited number of probe compounds. It would be interesting to test whether similar selectivity exists for ozone-resistant carboxylates with more complicated structures as well as catalytic ozonation with other metal oxides.

Acknowledgements

We acknowledge Dr. Haibo Zhu of KAUST Catalysis Center for his help in performing BET surface area analysis, Mr. Qingxiao Wang of

Imaging and Characterization Laboratory of KAUST for EDX analysis, Ms. Tong Zhan of WDRC for ICP-MS analysis, and Dr. Leonardo Gutierrez of University of Illinois at Urbana-Champaign for revising the English of this manuscript. We also appreciate the anonymous reviewers' valuable revision suggestions.

Appendix A. Supplementary data

Supplementary data associated with this article can be found, in the online version, at <http://dx.doi.org/10.1016/j.apcatb.2013.08.023>.

References

- [1] J. Nawrocki, B. Kasprzyk-Horden, *Appl. Catal. B* 99 (2010) 27–42.
- [2] T. Zhang, C. Li, J. Ma, H. Tian, Z. Qiang, *Appl. Catal. B* 82 (2008) 131–137.
- [3] L. Yang, C. Hu, Y. Nie, J. Qu, *Environ. Sci. Technol.* 43 (2009) 2525–2529.
- [4] L. Zhao, Z. Sun, J. Ma, *Environ. Sci. Technol.* 43 (2009) 4157–4163.
- [5] M. Sui, J. Liu, L. Sheng, *Appl. Catal. B* 106 (2011) 195–203.
- [6] T. Zhang, W. Li, J.P. Croué, *Environ. Sci. Technol.* 45 (2011) 9339–9346.
- [7] T. Zhang, W. Li, J.P. Croué, *Appl. Catal. B* 121/122 (2012) 88–94.
- [8] U. von Gunten, *Water Res.* 37 (2003) 1443–1467.
- [9] Y. Lee, *Environ. Eng. Res.* 11 (2006) 293–302.
- [10] T. Zhang, J. Lu, J. Ma, Z. Qiang, *Water Res.* 42 (2008) 1563–1570.
- [11] R. Larson, A. Rockwell, *Environ. Sci. Technol.* 13 (1979) 325–329.
- [12] I. Mazzarino, P. Piccinini, *Chem. Eng. Sci.* 54 (1999) 3107–3111.
- [13] H. Lee, D. Kang, J. Chi, D.H. Lee, *Korean J. Chem. Eng.* 20 (2003) 503–508.
- [14] N. Quici, M.E. Morgada, R.T. Gettar, M. Bolte, M.I. Litter, *Appl. Catal. B* 71 (2007) 117–124.
- [15] S. Raja, R. Dhanasekar, *Int. J. Chem. Technol. Res.* 3 (2011) 1926–1931.
- [16] I.A. Mudunkotuwa, V.H. Grassian, *J. Am. Chem. Soc.* 132 (2010) 14986–14994.
- [17] M.A. Blesa, A.D. Weisz, P.J. Morando, J.A. Salftly, G.E. Magaz, A.E. Regazzoni, *Coord. Chem. Rev.* 196 (2000) 31–63.
- [18] D.S. Pines, D.A. Reckhow, *Environ. Sci. Technol.* 36 (2002) 4046–4051.
- [19] F.J. Beltran, F.J. Rivas, R. Montero-de-Espinosa, *Ind. Eng. Chem. Res.* 42 (2003) 3218–3224.
- [20] R. Andreozzi, V. Caprio, A. Insola, R. Marotta, V. Tufano, *Water Res.* 32 (1998) 1492–1496.
- [21] P.M. Alvarez, F.J. Beltran, J.P. Pocostales, F.J. Masa, *Appl. Catal. B* 72 (2007) 322–330.
- [22] F. Delanoe, B. Acedo, N.K. VelLeitner, B. Legube, *Appl. Catal. B* 29 (2001) 315–325.
- [23] F.J. Beltran, F.J. Rivas, R. Montero-de-Espinosa, *Water Res.* 39 (2005) 3553–3564.
- [24] J. Hoigne, H. Bader, *Water Res.* 17 (1983) 185–194.
- [25] R.L. Wilson, C.L. Greenstock, G.E. Adams, R. Wageman, L.M. Dorfman, *Int. J. Radiat. Phys. Chem.* 3 (1971) 211–220.
- [26] G.V. Buxton, C.L. Greenstock, W.P. Helman, A.B. Ross, *J. Phys. Chem. Ref. Data* 17 (1988) 513–886.
- [27] T. Schaefer, J. Schindelfka, D. Hoffmann, H. Herrmann, *J. Phys. Chem. A* 116 (2012) 6317–6326.
- [28] W. Li, Z. Qiang, T. Zhang, X. Bao, X. Zhao, *J. Mol. Catal. A* 348 (2011) 70–76.
- [29] G.B. Deacon, R.J. Phillips, *Coord. Chem. Rev.* 33 (1980) 227–250.
- [30] G.B. Deacon, F. Huber, R.J. Phillips, *Inorg. Chim. Acta Art. Lett.* 104 (1985) 41–45.

- [31] O.W. Duckworth, S.T. Martin, *Geochim. Cosmochim. Acta* 65 (2001) 4289–4301.
- [32] A.D. Weisz, L.G. Rodenas, P.J. Morando, A.E. Regazzoni, M.A. Blesa, *Catal. Today* 76 (2002) 103–112.
- [33] F.P. Rotzinger, J.M. Kesselman-Truttmann, S.J. Hug, V. Shklover, M. Gratzel, *J. Phys. Chem. B* 108 (2004) 5004–5017.
- [34] S.J. Hug, D. Bahnemann, *J. Electron Spec. Rel. Phen.* 150 (2006) 208–219.
- [35] M. Menelaou, C. Mateescu, H. Zhao, I. Rodriguez-Escudero, N. Lalioti, Y. Sanakis, A. Simopoulos, A. Salifoglou, *Inorg. Chem.* 48 (2009) 1844–1856.
- [36] S. Hong, S.M. Huber, L. Gagliardi, C.C. Cramer, W.B. Tolman, *J. Am. Chem. Soc.* 129 (2007) 14190–14192.